Received: 18 February 2025 | Revised: 9 April 2025 | Accepted: 21 April 2025 | Published online: 6 May 2025

RESEARCH ARTICLE

Smart Wearable Technology
2025, Vol. 00(00) 1–9
DOI: 10.47852/bonviewSWT52025433

BON VIEW PUBLISHING

Study of a Visual Measurement System for Woven Grids

Hufeng Zou[1], Quanyu Wu[1,*], Zehan Ye[2], Jiaqi Fan[1], Lingjiao Pan[1] and Xiaojie Liu[1]

[1]*School of Electrical and Information Engineering, Jiangsu University of Technology, China*

[2]*College of Marine Engineering, Jimei University, China*

Abstract: In order to solve the problems of low efficiency and poor accuracy in measuring the geometrical parameters of braided pipe mesh by traditional methods, an improved method for measuring the geometrical parameters of braided pipe is proposed. The method acquires the braided pipe grid image by a CMOS camera and reduces the influence of color and noise on the image quality by using preprocessing means such as grayscaling and bilateral filtering. Subsequently, the region of interest of the woven tube grid structure is extracted from the background using an iterative method, and the average filament diameter is calculated by Canny edge detection and a modified Hough transform. Next, the skeleton wire segment contours are obtained using the skeleton operator, and the contours are further optimized by the RDP algorithm to retain only the straight line segments. The co-linear straight line segments are connected to form a complete mesh line by a contour merging operation. Finally, the mesh size is indirectly obtained using the improved least-squares method based on feature classification. Through experimental verification, the method has a practical value as it improves the average wire diameter accuracy by 3% and the mesh size accuracy by 1% compared with the traditional machine vision measurement method.

Keywords: machine vision, woven tube, improved Hough transform, skeleton profile optimization

1. Introduction

With the continuous advancement of machine vision technology and its widespread application in product dimension inspection, this non-contact measurement method has gained increasing attention in the field of dimensional measurement due to its significant advantages. Machine vision can not only be used to measure the dimensions of parts but also to capture the geometric parameters of fine mesh structures. The continuous improvement of digital image processing and pattern recognition technologies has greatly promoted the application and development of machine vision in dimensional measurement.

Compared to traditional methods of manufacturing tubular materials such as winding and extrusion molding, weaving can accommodate objects of various shapes and form woven structures of different configurations. It is now widely used in fields such as healthcare and aerospace. The mesh parameters in woven tubes are one of the key factors influencing their performance and applicability.

Different mesh parameters may result in varying physical properties, flexibility, insulation, flame retardancy, and more. Therefore, high precision in the dimensions of woven meshes is required in practical applications. Using measuring tools like micrometers and vernier calipers to measure the geometric parameters of woven meshes often involves issues such as significant human subjective influence, low reliability, and low efficiency, making it difficult to meet the need for real-time feedback on measurement results. As a result, machine vision measurement methods have gradually begun to replace traditional manual measurement methods [1, 2].

In recent years, scholars both domestically and internationally have conducted extensive research on the measurement of geometric parameters of woven meshes. Wang et al. [3] achieved edge point extraction and fitting of woven meshes using an image measurement instrument and conducted research on the calculation of mesh hole spacing and automatic search. Tang et al. [4] proposed an automatic measurement system for woven mesh test sieves based on image processing. After capturing images using a CCD camera, the system processed the images through software for preprocessing operations and obtained the dimensional parameters of the woven mesh.

Zhao [5] proposed a measurement scheme based on image measurement technology to improve the detection efficiency of image measuring instruments. Using the Hough algorithm, he obtained the average wire diameter of the metal woven mesh and, based on Canny edge detection and the maximum bounding rectangle, determined the largest mesh hole size. Liu [6] proposed an automatic detection method for test sieves based on image measuring instruments, which mainly involves edge capturing, edge fitting, and obtaining sieve hole data to achieve test sieve calibration results. Although the above traditional computer vision methods already have an error of less than 7% for metal wires with a wire diameter of about 0.01 mm, in certain application scenarios where high precision is required, such as in medical and aerospace fields, an error of 1 μm may still affect the performance

*Corresponding author: Quanyu Wu, School of Electrical and Information Engineering, Jiangsu University of Technology, China. Email: wuquanyu@jsut.edu.cn

of the product. Therefore, further improvement of measurement accuracy is necessary.

To improve the measurement efficiency and accuracy of the geometric parameters of woven tube meshes, an improved measurement method has been proposed. This method involves capturing images of the woven tube using a CMOS camera, followed by image preprocessing including grayscaling, bilateral filtering, and iterative threshold segmentation to extract the region of interest (ROI) within the woven mesh structure. After extracting the edge contours of the mesh structure using the Canny algorithm, the average wire diameter of the woven mesh is measured through an improved Hough transform. Since the shape of a single mesh hole is unstable, and to enhance measurement accuracy, the average hole spacing is used to indirectly obtain the hole size. The skeleton operator is applied to the ROI to obtain the skeleton line contours. Using the Ramer–Douglas–Peucker (RDP) algorithm, the skeleton contours are simplified to retain only the straight line segments. By merging the contours and connecting collinear lines, the central axis line of each mesh is obtained. The average hole spacing between adjacent metal wires is then calculated using an improved least-squares method based on feature classification. The mesh hole size is determined by the difference between the hole spacing and the wire diameter. Finally, the real size of the woven tube mesh is obtained through camera size calibration. A comparison between the proposed improved method and traditional machine vision measurement methods shows that the improved method provides higher accuracy in measuring the geometric parameters of woven tube meshes.

2. Braided Mesh Size Measurement Requirements and Measurement System

2.1. Measurement requirements

China Industrial Metal Screen Mesh and Wire Woven Wire Mesh (GB/T 5330.1-2012) and Industrial Wire Woven Wire Mesh Technical Requirements and Inspection (GB/T 17492-1998) provide definitions of mesh size ω, wire diameter d, and pitch p of industrial metal wire braided meshes [7].

Mesh size refers to the distance between two adjacent metal wires. Wire diameter d is the diameter of the metal wire on the braided mesh. Pitch p is the sum of the mesh size and wire diameter, as shown in Figure 1. This paper focuses on measuring mesh size ω and wire diameter d, as they jointly determine the performance of the screen. When designing or selecting braided mesh, it is essential to consider the relationship between mesh size and wire diameter.

Figure 1
Mesh size, wire diameter, and pitch

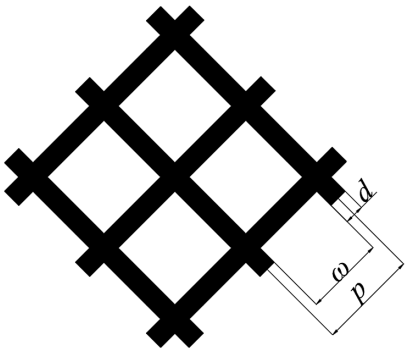

2.2. Measurement system

The measurement system consists of hardware and software components. The hardware configuration is shown in Figure 2. A Hikvision 5-megapixel industrial camera is selected as the image acquisition device, paired with a Light Tiger OTL11.5-05-110C telecentric lens to ensure high-precision imaging. Additionally, a parallel backlight is used to optimize image quality, a high-performance computer is used to process data, network cables ensure stable image data transmission, and a sample platform is used to fix the optical equipment.

Regarding software, the development is done using HALCON 20.11 combined with Qt 6.5.1. First, HALCON's powerful image processing capabilities are used to preprocess and analyze the dimensions of the captured braided tube images. Then, key algorithms from this process are converted into C++ code for further integration. Finally, within the Qt framework, a complete braided tube size measurement function is achieved by calling the Application Programming Interfaces provided by HALCON. This solution is both efficient and user-friendly, significantly enhancing the flexibility and scalability of the entire system.

Figure 2
Braided tube mesh size detection hardware platform

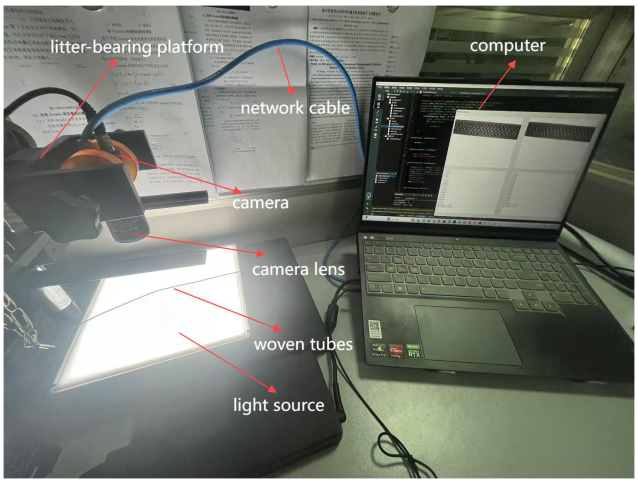

The measurement process of braided tube mesh size is shown in Figure 3. The specific process is as follows:

1) Image Acquisition and Preprocessing: First, the braided tube image is captured, and then grayscale conversion and image filtering are applied to reduce the impact of color and noise. The iterative method in automatic threshold segmentation is used to extract the braided mesh area.
2) Average Wire Diameter Measurement: The Canny algorithm is used to obtain the edge contours of the braided mesh, and the DBSCAN-based Hough transform is used to fit straight lines along both edges of a single mesh line. The average wire diameter is calculated based on the distance between these lines.
3) Calculate the Average Hole Distance: The skeleton wire segment contour is obtained using the skeleton operator in HALCON, the

Figure 3
Braided tube mesh size detection flowchart

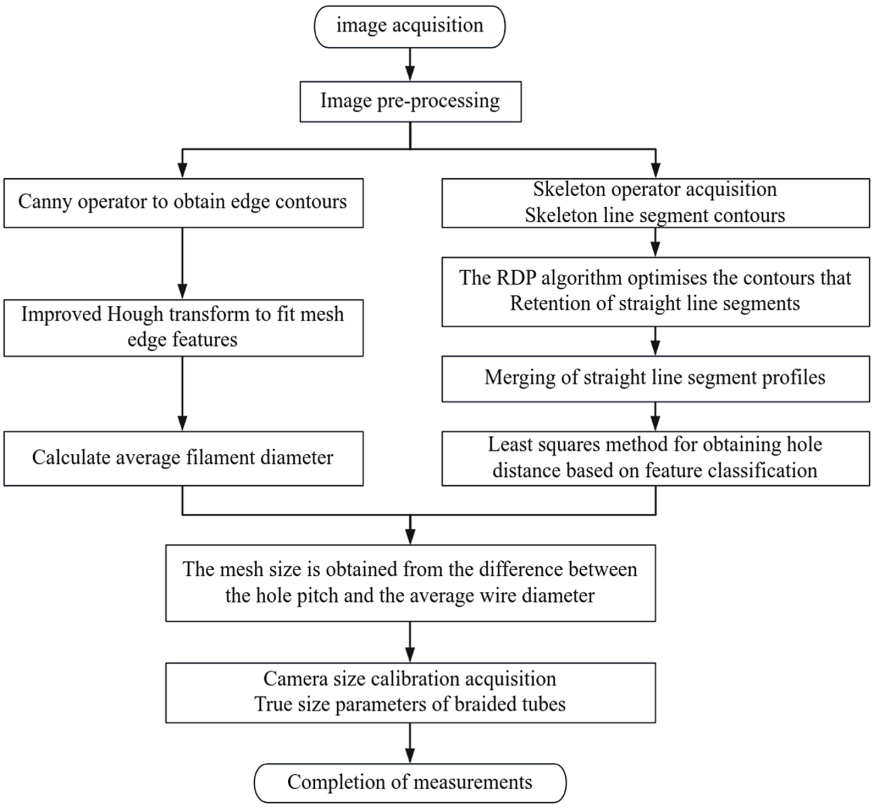

contour is simplified by the RDP algorithm to remove more than the contour interference to retain only the straight line segments and then connected to the common straight line by the union_collinear_contours_xld operator in HALCON, and finally, the neighboring wires are obtained by the improved least-squares method based on the classification of the characteristics of the average hole distance.

4) Mesh Hole Size Calculation: The mesh hole size is calculated using the difference between average pitch and average wire diameter. A calibration plate is used to obtain the pixel-to-real size conversion factor (P) in the image. Using this conversion factor, the true size of the braided tube mesh is calculated.

3. Measurement of Woven Mesh Geometric Parameters

3.1. Image preprocessing

3.1.1. Grayscale processing

Using a Hikvision camera to capture images of the woven tube, in order to eliminate the impact of color on the woven mesh features, the image is converted to grayscale using a weighted averaging method [8], as shown in Equation (1):

$$Gray = 0.299 \times R + 0.587 \times G + 0.144 \times B \tag{1}$$

where R, G, and B represent the values of the red, green, and blue channels, respectively, and their coefficients correspond to the perceived weights of red, green, and blue by the human eye.

3.1.2. Filtering processing

Noise reduction processing is used to remove the grayscale variations in the non-edge regions of the image, which can effectively suppress the interference of noise on image features. Bilateral filtering, by combining Gaussian weights in both the spatial domain and the grayscale domain, can effectively smooth the noise while preserving image edges, achieving edge-preserving denoising. This method not only suppresses the grayscale variations in non-edge regions and reduces noise interference but also avoids the edge blurring problem caused by traditional filtering methods, thus maintaining the integrity of image feature information [9]. The principle is as follows:

$$q = \frac{\sum_{i \in S} I(i) \cdot \omega(i,p)}{\sum_{i \in S} \omega(i,p)} \tag{2}$$

$$\omega(i,p) = g_s(\|p - i\|) \cdot g_r(|I(p) - I(i)|) \tag{3}$$

In the equation, q is the output value after bilateral filtering; p is the given pixel point; $I(i)$ is the original grayscale of the neighboring pixel i; S is the neighborhood of pixel p; $\omega(i,p)$ is the bilateral filtering weight from pixel i to pixel p; $g_s(\|p - i\|)$ is the spatial domain Gaussian function; and $g_r(|I(p)| - |I(i)|)$ is the range Gaussian function. Figure 4(b) shows the woven tube image after bilateral filtering.

3.1.3. Threshold segmentation

The iterative method is used to separate the foreground and background from a grayscale image, and the distinction between foreground and background is optimized by continuously adjusting the threshold value until a certain convergence condition is satisfied. According to the literature [10], the iterative

thresholding method is a commonly used image segmentation method with the following procedure:

Step 1: Determine the initial threshold using the mean of the image grayscale, as shown in Equation (4), where M and N are the number of rows and columns of the image and *I(i, j)* is the pixel value at position *(i, j)*:

$$T_0 = \frac{1}{MN}\sum_{i=0}^{M-1}\sum_{j=0}^{N-1} I(i,j) \tag{4}$$

Step 2: Using the current threshold T_k, classify each pixel in the image. If $I(i, j) > T$, the pixel is considered as foreground; otherwise, it is considered as background.

Step 3: Based on the segmentation result from Step 2, calculate the average grayscale values of the foreground μ_F and μ_B background, as shown in Equation (5), where N_f and N_b represent the number of foreground and background pixels, respectively:

$$\begin{cases} \mu_F = \dfrac{\sum_{I(i,j)>T_k} I(i,j)}{n_F} \\ \mu_B = \dfrac{\sum_{I(i,j)\le T_k} I(i,j)}{n_B} \end{cases} \tag{5}$$

Step 4: Update the threshold. The new threshold T_{k+1} is taken as the median of the average grayscale values of the foreground and background, $T_{k+1} = 0.5 \times (\mu_F + \mu_B)$.

Step 5: Check if the difference between the new threshold T_k and the previous threshold T_{k+1} is smaller than a preset value (0.05). If it is $|T_{k+1} - T_k| < \varepsilon$, stop the iteration, and the final threshold is the optimal value T_{k+1}; otherwise, return to Step 2 and continue the iteration.

Step 6: When the algorithm converges, perform binary thresholding on the image using the final threshold *T*. If the current pixel value is greater than *T*, it is output as 0 (foreground); otherwise, it is output as 255 (background).

To determine the optimal automatic thresholding method, experiments were conducted to compare the iterative method, Otsu's method (maximum between-class variance), and the K-means method. The experimental results are shown in Figure 4(c)–(e). From the results, it is clear that the iterative method can more clearly extract the woven grid structure. Therefore, the iterative method is chosen for automatic thresholding [10].

3.2. Woven mesh wire diameter measurement

In digital images, edges refer to the set of pixels where there is a significant change in grayscale values. Edge detection, as a fundamental algorithm, plays a crucial role in digital image analysis and target feature extraction. The Canny edge detection operator is widely used due to its excellent signal-to-noise ratio, precise localization ability, single response characteristic, and the ability to effectively distinguish between true edges and noise through multi-level thresholding. Therefore, the Canny algorithm is used to locate the edges of woven metal wires in the mesh [11–13], as shown in the detection result in Figure 5(a).

The Hough transform is a feature extraction technique used to detect simple shapes such as lines and circles in an image. It is particularly suitable for handling cases with noise and discontinuities but is not ideal for situations with a large number of abrupt changes (discontinuities).

The traditional machine vision method for measuring wire diameters involves using the Hough transform to directly fit edge

Figure 4
Woven tube image preprocessing. (a) Woven tube image. (b) Bilateral filter image. (c) Iterative thresholding segmentation. (d) Otsu's thresholding. (e) K-means thresholding segmentation

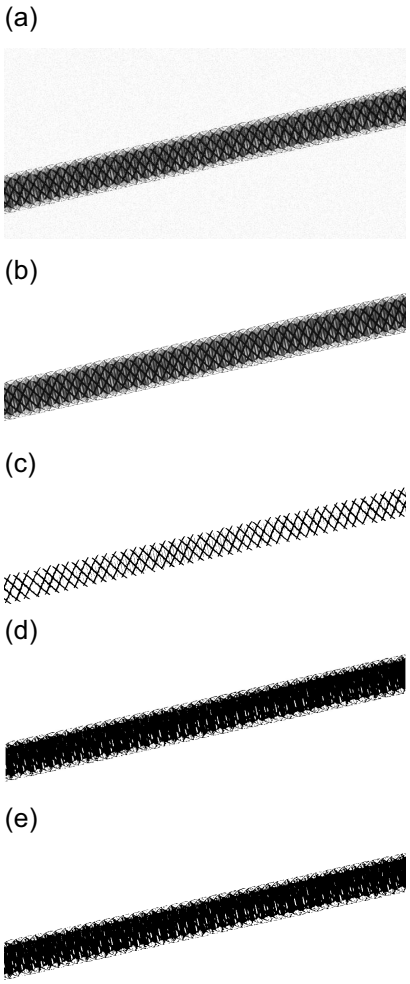

line features. However, as shown in Figure 5(a), the edge contours of the woven mesh reveal that the metal wire edges often exhibit discontinuities due to overlapping, and there are many abrupt points causing the contours to have irregularities. These abrupt points can affect the fitting accuracy of the Hough transform. Therefore, in this study, the DBSCAN algorithm is introduced to filter out these abrupt points, enabling the Hough transform to better fit the true edge of the metal wire. The fitting results are shown in Figure 5(b), and the specific fitting measurement process is as follows [14]:

Step 1: Construct the edge point set *M* of the woven mesh. Set the number of iterations for the DBSCAN algorithm n = 100 and the inlier threshold d = 3. Initialize the best model parameters best_model and the maximum number of inliers max_inliers to 0.

Step 2: For each iteration, randomly select two points (x_1, y_1), (x_2, y_2) from the point set *M* to determine the model parameters. Use these two points to compute a hypothesis line model $y = mx + b$. Then, iterate through the entire point set (x_i, y_i), calculating the perpendicular distance from each point to the line d_i, $d_i = |y_i - (mx_i + b)| / \sqrt{1+m^2}$. If the distance is smaller than the threshold $d_i = 3$, consider that point as an inlier. If the number of inliers found in this iteration exceeds the previously recorded maximum number of inliers, update the best model parameters best_model and the

Figure 5
Measurement of the diameter of braided pipe wires. (a) Canny edge detection. (b) Improved Hough transform for line fitting

(a)

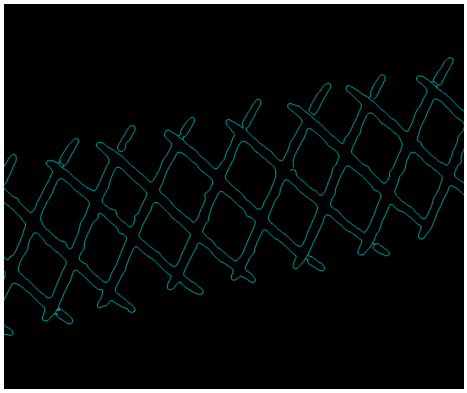

(b)

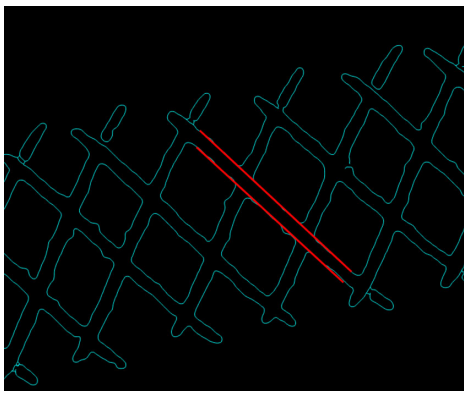

maximum number of inliers max_inliers, and add all inliers to the new point set *N*.

Step 3: After all iterations, the best_model will represent the final estimated best model parameters. All points identified as inliers are considered non-discrete points, and the point srt N will be the non-discrete point set.

Step 4: Use the Hough transform to fit a line to all points in the non-discrete point set *N*. Create a line equation $r = x\cos\theta + y\sin\theta$ and a 2D array *S* to serve as an accumulator. Iterate through each point in the point set *N*, considering a range of possible values for the parameters of the line (typically angle θ and distance *r*). For each point, compute the corresponding *r* value. Then, increment the count at the corresponding position in the accumulator array *S*. After processing all points, identify the element in the accumulator with the highest count. The corresponding *(r, θ)* values for $m = -\cos\theta \,/\, \sin\theta$ and $b = r \,/\, \sin\theta$ define the line, which can then be converted into the standard line equation $y = mx + b$.

3.3. Measurement of woven mesh hole spacing

As shown in Figure 6, the traditional machine vision measurement method for woven mesh hole size involves randomly selecting several mesh holes, performing preprocessing to obtain the mesh structure, and then fitting the mesh hole edge feature lines using feature fitting methods to acquire the average hole spacing. However, due to the inconsistency in hole sizes, this method has a high degree of randomness, leading to inaccurate

Figure 6
Traditional mesh hole size measurement method

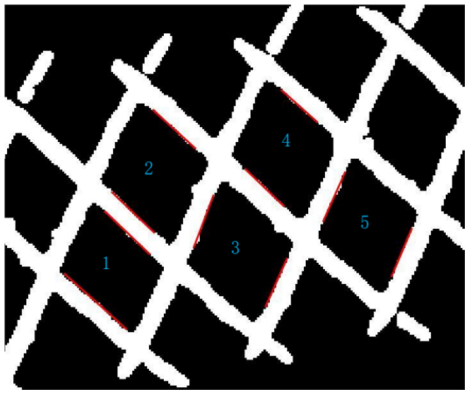

results. Therefore, in order to improve measurement accuracy, this paper proposes a method to indirectly obtain the hole size by calculating the average distance between adjacent metal wires (i.e., the average hole spacing).

3.3.1. Metal wire centerline profile extraction

In image processing, skeletonization, also known as centerline extraction, aims to reduce the shape of an object to a thin structure composed of lines. These lines preserve the key features of the original shape while greatly reducing data volume. To extract the centerline of the metal wires from the segmented mesh structure, the skeleton of the mesh structure is extracted. This is achieved by using the skeleton operator in HALCON to extract the mesh structure's skeleton and then converting it into a subpixel contour using the gen_contours_skeleton_xld operato [15].

The extracted skeleton contours often contain a significant amount of noise lines, which can greatly interfere with centerline fitting. In this paper, the RDP algorithm is used to filter out the noise lines. The RDP algorithm is an iterative method for curve simplification, which reduces the number of points defining a curve while retaining the key shape characteristics of the original curve. When processing skeleton contours, the RDP algorithm can be used to preserve the main straight segments. The algorithm principle is illustrated in Figure 7, and the simplification process is as follows [16, 17]:

Figure 7
The principle diagram of the RDP (Ramer–Douglas–Peucker) algorithm

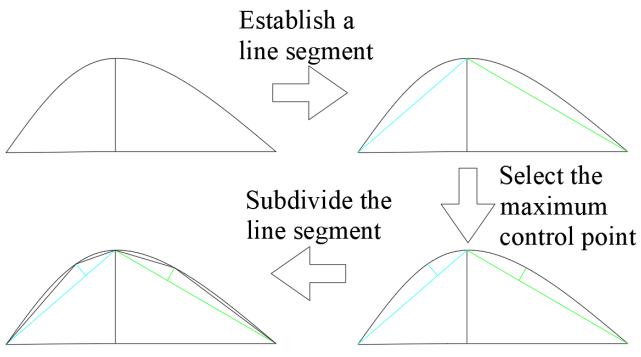

1) Process 1: Construct a skeleton contour point set P, and set ϵ the approximation threshold.
2) Process 2: Calculate the straight line segment L between the start point $P_{[0]}$ and the end point $P_{[n-1]}$. Traverse through each point $P_{[i]}$ in the point set P, calculate the distance d from point $P_{[i]}$ to the straight line segment L, and find the point $P_{[k]}$ with the maximum distance. If $d > \varepsilon$ threshold, connect the point with the start point $P_{[0]}$ and end point $P_{[n-1]}$, forming new approximation line segments L_1 and L_2. Continue calculating the distances until $d < \varepsilon$ threshold.
3) Process 3: When a segment of the contour points satisfies the straight-line equation $y = mx + b$, that segment of the contour is divided into a straight line. If it does not satisfy the straight-line equation, that segment of the contour is discarded.

In this paper, to achieve a more ideal segmentation result, the RDP algorithm is used in a coarse-to-fine manner for skeleton contour segmentation. The resulting effect is shown in Figure 8(b). First, a high threshold ε_{max} is used for contour approximation to segment out larger straight-line contours, and then a low ε_{min} threshold is applied to further refine and segment smaller straight-line contours. Compared to a single segmentation, this method produces a more ideal segmentation result.

After segmentation using the RDP algorithm, the skeleton contours often exhibit numerous discontinuities. Although an improved Hough transform can be used to fit straight lines, the large number of metal wires in the image and the relatively high computational cost of the Hough transform make it less efficient. Therefore, to address this issue, the discontinuous contours are merged, and the faster least-squares method is applied for fitting. The union_collinear_contours_xld operator is used to connect the collinear contours. The resulting skeleton contours after merging the collinear contours are shown in Figure 8(c). This method effectively connects the discontinuous collinear contours, forming the centerline contours of the metal wires.

3.3.2. Calculation of average hole spacing

To facilitate the calculation, after fitting the metal wire centerline contours into straight lines using the improved least-squares method [18–21], the centerlines are classified based on different winding directions. The straight lines with positive slopes are shown in Figure 9(a), and those with negative slopes are shown in Figure 9(b). The average hole distance calculation process is as follows:

Step 1: Place all the centerline contours into an empty template M, and initialize the templates leftlines and rightlines.

Step 2: Select the first contour M_1 from the template M, and place it into the corresponding initialized template based on its direction. Obtain its contour point set P. Then, use the DBSCAN algorithm to traverse each point P_i in the point set. The non-abrupt change points are added to the point set Q, and through Equations (6)–(10), the straight line l_i that best fits the point set Q is calculated.

$$l_1 = \sum_{i=1}^{n} [y_i - (mx_i + b)]^2 \tag{6}$$

$$\frac{\partial l_1}{\partial m} = -2\sum_{i=1}^{n} x_i[y_i - (mx_i + b)] = 0 \tag{7}$$

$$\frac{\partial l_1}{\partial b} = -2\sum_{i=1}^{n} [y_i - (mx_i + b)] = 0 \tag{8}$$

Figure 8
Metal wire centerline contour extraction. (a) Skeleton contour. (b) RDP segmentation. (c) Contour merging

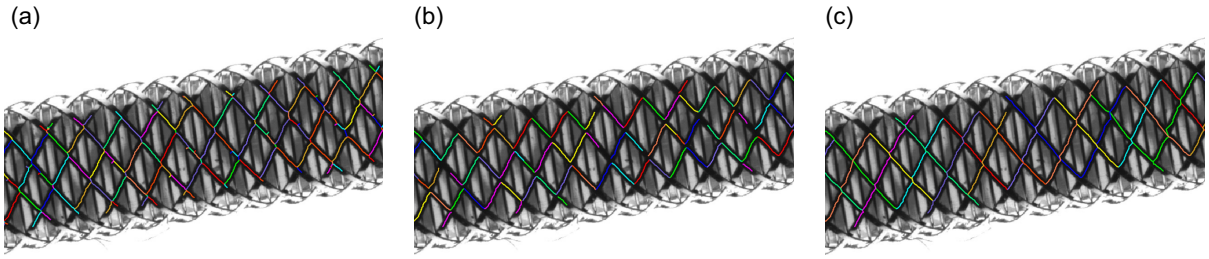

Figure 9
Metal wire centerline classification. (a) Positive slope centerline. (b) Negative slope centerline

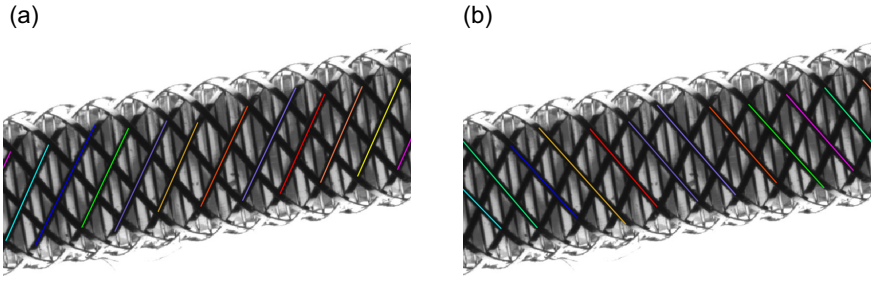

$$m = \frac{n\sum_{i=1}^{n} x_i y_i - \sum_{i=1}^{n} x_i - \sum_{i=1}^{n} y_i}{n\sum_{i=1}^{n} x_i^2 - (\sum_{i=1}^{n} x_i)^2} \tag{9}$$

$$b = \frac{\sum_{i=1}^{n} y_i - m\sum_{i=1}^{n} x_i}{n} \tag{10}$$

Step 3: Sequentially select other contours M_i from the template M, and fit them into straight lines l_i using the same principle as in Step 2. Then, use the angel_II operator to calculate the angle θ_i between each line l_i and l_1. Based on the judgment criteria $0 \leq \theta_i \leq 20°$, if the condition is met, the line is considered to be in the same direction as l_1 and is placed in the same template; otherwise, it is placed in a different template.

Step 4: Sequentially calculate the average distance between adjacent centerlines in the templates lifelines and rightlines. Finally, calculate the average of the average distances obtained from the two templates, which will be used as the average hole distance between the metal wires.

3.4. Camera size calibration

The wire diameter and hole distance of the woven grid obtained through the image processing and feature extraction described above are in pixels. To obtain the actual dimensions, a standard 5.000 mm circular gauge block is measured using the designed system, resulting in 103.6967 pixels. Therefore, the system's dimension conversion unit P is 0.009644 mm/pixel.

4. Experimental Verification

The designed system is used to capture images of a braided tube with a wire diameter of 0.01 mm and a mesh hole size of 0.04. The image processing and feature extraction methods described above are used to measure the geometric parameters of the braided tube mesh. As shown in Figure 10, by measuring the wire diameter at three locations, the average wire diameter is obtained as 0.01023 mm,

Figure 10
Braided tube mesh size measurement

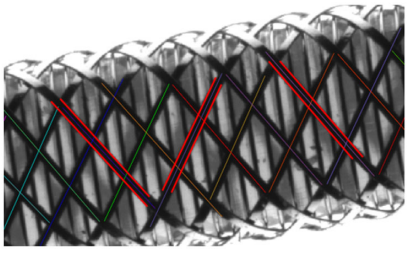

with a measurement error of 2.3% compared to the actual wire diameter. The average hole distance is calculated as 0.04977 mm by measuring the average distance between two sets of centerlines in different directions. The mesh hole size is obtained as 0.03954 mm by calculating the difference between the hole distance and wire diameter, with an error of 1.15% compared to the actual mesh hole size.

Zhao [5], in his article "Research on Image Measurement Techniques in the Calibration of Test Sieves," measured wire parameters by traditional machine vision methods. Traditional machine vision measurement methods directly fit edge features through the Hough transform for measuring wire diameter. For measuring mesh hole size, several grids are randomly selected, and their average size is taken as the final mesh hole size. To verify whether the accuracy of the method described in this paper is improved compared to traditional machine vision measurement methods, the measurement results are compared. To eliminate the possibility of measurement errors due to chance, four groups of measurements are conducted on different regions of the braided tube with a wire diameter of 0.01mm and a mesh hole size of 0.04, as shown in Figure 11. The wire diameter measurement results for

Figure 11
Four region images of the braided tube

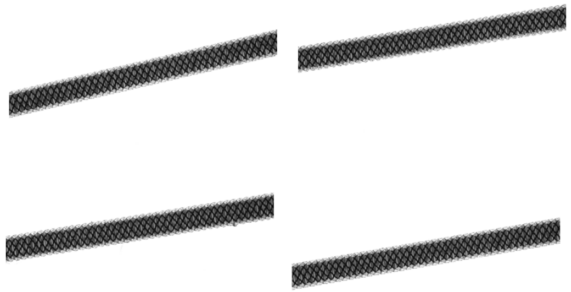

the two methods are shown in Table 1; the hole distance measurement results for the method described in this paper are shown in Table 2, and the mesh hole sizes calculated by this method and measured by the traditional method are shown in Table 3.

Table 1
Average wire diameter measurement results

Number	Method	Average wire diameter	Error
1	Our Approach	0.01017 mm	1.7%
1	Traditional Method	0.01045 mm	4.5%
2	Our Approach	0.01025 mm	2.5%
2	Traditional Method	0.01067 mm	6.7%
3	Our Approach	0.01013 mm	1.3%
3	Traditional Method	0.01035 mm	3.5%
4	Our Approach	0.01016 mm	1.6%
4	Traditional Method	0.01042 mm	4.2%

Table 2
Average hole diameter measurement results

Number	Method	Average hole distance
1	Our Approach	0.04971 mm
2	Our Approach	0.04954 mm
3	Our Approach	0.04985 mm
4	Our Approach	0.04982

As shown in Table 1, for wire diameter measurement, the DBSCAN algorithm filters out discrete points, resulting in a fitted feature that is closer to the edge. This leads to an improvement of about 3% in the measurement accuracy of the wire diameter using the method described in this paper compared to the traditional

Table 3
Mesh hole size measurement results

Number	Method	Mesh hole size	Error
1	Our Approach	0.03954 mm	1.15%
1	Traditional Method	0.04086 mm	2.15%
2	Our Approach	0.03929 mm	1.78%
2	Traditional Method	0.04097 mm	2.43%
3	Our Approach	0.03965 mm	0.88%
3	Traditional Method	0.04104 mm	2.6%
4	Our Approach	0.03966 mm	0.85%
4	Traditional Method	0.04075 mm	1.875%

method. According to Tables 2 and 3, the method of indirectly obtaining the mesh hole size by calculating the average hole distance and average wire diameter has an accuracy improvement of about 1% compared to the traditional method, which directly measures the average mesh hole size. In conclusion, the method presented in this paper shows a certain improvement in accuracy compared to traditional measurement methods.

5. Conclusion

Aiming at the limitations of the traditional machine vision measurement method in measuring the geometric parameters of braided tubes, this study proposes an improved measurement method and verifies its effectiveness through experiments. First, in terms of braided mesh area segmentation, the iterative method, Otsu method, and K-means method are compared, and the results show that the iterative method is able to segment a clearer braided mesh structure. Second, the DBSCAN-based Hough transform is used for average wire diameter measurement, which effectively reduces the interference of mutation points and significantly improves the measurement accuracy. In addition, accurate measurement of average aperture distance between adjacent wires is achieved by skeleton optimization and improved least squares based on feature classification. In terms of mesh size measurement, the indirect measurement method combining the average aperture distance and the average conductor diameter has higher accuracy compared with the direct measurement. Experimental results show that the error of the average wire diameter measured by this method is less than 3% and the error of the mesh size is less than 2%, which is significantly better than the traditional measurement method. The improved method proposed in this study shows good practicality and high measurement accuracy in the field of woven wire mesh inspection.

Acknowledgments

This research is funded by the Changzhou Social Development Project CE20225045 and the industry–university research cooperation project KYH24087.

Ethical Statement

This study does not contain any studies with human or animal subjects performed by any of the authors.

Conflicts of Interest

The authors declare that they have no conflicts of interest to this work.

Data availability statement

Data sharing is not applicable to this article as no new data were created or analyzed in this study.

Author Contribution Statement

Hufeng Zou: Conceptualization, Methodology, Investigation, Data curation, Writing – original draft, Writing – review & editing, Visualization. **Quanyu Wu:** Validation, Formal analysis, Resources, Writing – review & editing, Project administration. **Zehan Ye:** Investigation, Resources, Writing – original draft, Writing – review & editing. **Jiaqi Fan:** Software. **Lingjiao Pan:** Writing – review & editing. **Xiaojie Liu:** Supervision.

References

[1] Zhou, Y. (2021). Jīnshǔsī biānzhīwǎng shìyànshāi jiàozhǔn de zhùyì shìxiàng [Matters needing attention in calibration of wire woven test sieve]. *Modern Manufacturing Technology and Equipment*, *57*(5), 144–145. https://doi.org/10.16107/j.cnki.mmte.2021.0401

[2] Shi, Z., & Hu, J. (2024). Biānzhīguǎn de jiégòu, gōngyì jí xìngnéng yánjiū jìnzhǎn [Research progress on the structure, technology and performance of braided tubes]. *Advanced Textile Technology*, *32*(12), 113–122. https://doi.org/10.19398/j.att.202403003

[3] Wang, X., Niao, Z., Yang, C., Qian, Z., & Chen, H. (2013). Jīyú yǐngxiàng cèliángyí de shìyànshāi zìdòng cèliáng fāngfǎ [Calibration method for test sieves based on video measuring machine]. *Journal of Data Acquisition & Processing*, *28*(2), 257–260. https://doi.org/10.16337/j.1004-9037.2013.02.002

[4] Tang, D., Shi, H., Fu, Y., Jiang, Z., & Zeng, Y. (2016). Jīyú túxiàng chǔlǐ jìshù de shìyànshāi zìdòng cèliáng xìtǒng [Automatic measuring system for test sieves based on image processing techniques]. *Shanghai Measurement and Testing*, *43*(1), 17–19.

[5] Zhao, Y. (2019). Shìyànshāi jiàozhǔn zhōng de túxiàng cèliáng jìshù yánjiū [Research of image measurement technology of test sieves' calibration]. *Ideo Engineering*, *43*(7), 11–15. https://doi.org/10.16280/j.videoe.2019.07.003

[6] Liu, Y. (2023). Jīyú yǐngxiàng cèliángyí de shìyànshāi zìdòng jiǎncè fāngfǎ yánjiū [Research on automatic detection method of test screen based on image measuring instrument]. *Industrial Measurement*, *33*(1), 19–23. https://doi.org/10.13228/j.boyuan.issn1002-1183.2022.0128

[7] Li, H., Yang, L., Yang, H., Wang, S., & Wang, P. (2022). Chāoxì jīnshǔsī biānzhī wǎngzhuàng cáiliào de xìngnéng hé yìngyòng [Properties and application of ultra-fine metalwire weaved mesh materials]. *Metallic Functional Materials*, *29*(6), 53–58. https://doi.org/10.13228/j.boyuan.issn1005-8192.20220109

[8] Huang, H., Guo, L., Zhou, X., Wu, Y., Wang, T., & Li, M. (2024). Jīyú jīqì shìjué de wēixiǎo chōngyā língjiàn chǐcùn cèliáng [Size measurement of tiny stamping parts based on machine vision]. *Application of Electronic Technique*, *50*(7), 59–64. https://doi.org/10.16157/j.issn.0258-7998.245057

[9] Hao, B., Xu, X., & Yan, J. (2024). Jīyú jīqì shìjué de mǎojiēkǒng jǐhé cānshù cèliáng [Measurement of rivet hole geometric parameters based on machine vision]. *Tool Engineering*, *58*(3), 131–137.

[10] Liu, G., Wang, S., Cao, Y., Zhao, E., Zhang, L., Su, L., & Xing, C. (2022). Jǐ zhǒng jīngdiǎn yùzhí fēngē fāngfǎ zài túxiàng

chǔlǐ zhōng de yìngyòng yánjiū [Application of several classical threshold segmentation methods in image processing]. *Journal of Huanggang Polytechnic*, *24*(4), 99–103.

[11] Zhang, H., Cheng, S., Zhao, Y., Jing, J., Su, Z., & Li, P. (2023). Measurement of yarn apparent evenness based on modified Canny edge detection. *The Journal of The Textile Institute*, *115*(4), 600–606. https://doi.org/10.1080/00405000.2023.2201997

[12] Song, Y., Li, C., Xiao, S., Zhou, Q., & Xiao, H. (2024). A parallel Canny edge detection algorithm based on OpenCL acceleration. *PLoS ONE*, *19*(1), e0292345. https://doi.org/10.1371/journal.pone.0292345

[13] Gayathri Monicka, S., Manimegalai, D., & Karthikeyan, M. (2022). Detection of microcracks in silicon solar cells using Otsu-Canny edge detection algorithm. *Renewable Energy Focus*, *43*, 183–190. https://doi.org/10.1016/j.ref.2022.09.002

[14] Du, L., Zhou, Z., & Wang, T. (2022). Jīyú jīqì shìjué de lǚhéjīn lúngǔ chǐcùn cèliáng [Dimension measurement of aluminum alloy hub based on machine vision]. *Journal of Machine Design*, *39*, 193–198. https://doi.org/10.13841/j.cnki.jxsj.2022.s2.033

[15] Li, Z., Yan, J., Fu, Q. & Liu, W. (2022). Jīyú jīqì shìjué de jīnshǔ gōngjiàn chǐcùn cèliáng [Dimension measurement of metal workpiece based on machine vision]. *Instrument Technique and Sensor*, (3), 92–97. https://doi.org/10.3969/j.issn.1002-1841.2022.03.018

[16] Luo, J., Huang, Q., Huang, J., & Cao, L. (2023). Miànxiàng hángkōng fādòngjī yèpiàn sǔnchǐ lúnkuò de chǐcùn cèliáng jìshù [Dimensional measurement technology for tenon tooth profile of aero-engine blades]. *Electronic Measurement Technology*, *46*(24), 139–148. https://doi.org/10.19651/j.cnki.emt.2314048

[17] Gu, L., & Wu, J. (2024). Jīyú jīqì shìjué zhuǎnzǐ chōngpiàn yà xiàngsù jīngdù chǐcùn cèliáng yánjiū [Research on sub-pixel precision dimension measurement of rotor punching based on machine vision]. *Computer Measurement & Control*, *32*(4), 29–36. https://doi.org/10.16526/j.cnki.11-4762/tp.2024.04.005

[18] Ren, C., Zhang, J., Yang, C., Song, W., & Wu, Z. (2024). Jīyú jīqì shìjué de mù chuāng shuāng duān xǐxiāo jiāgōng chě cùn cèliáng fǎngfǎ [Research on the dimensional measurement method of double end milling processing of wooden windows based on machine vision]. *Journal of Forestry Engineering*, *9*(1), 141–149. https://doi.org/10.13360/j.issn.2096-1359.202305007

[19] Zhang, B., Gao, J., Wang, J., & Liu, J. (2023). Jīyú jīqì shìjué de yuán xíng diànquān chǐcùn cèliáng xìtǒng shèjì [Design of measuring system for circular gasket size based on machine vision]. *Tool Engineering*, *57*(7), 141–145.

[20] Giannelli, C., Imperatore, S., Kreusser, L. M., Loayza-Romero, E., Mohammadi, F., & Villamizar, N. (2024). A general formulation of reweighted least squares fitting. *Mathematics and Computers in Simulation*, *225*, 52–65. https://doi.org/10.1016/j.matcom.2024.04.029

[21] Galbetti, M. V., Zuffo, A. C., Shinma, T. A., Boulomytis, V. T. G., & Imteaz, M. (2021). Evaluation of the tabulated, NEH4, least squares and asymptotic fitting methods for the CN estimation of urban watersheds. *Urban Water Journal*, *19*(3), 244–255. https://doi.org/10.1080/1573062X.2021.1992639

How to Cite: Zou, H., Wu, Q., Ye, Z., Fan, J., Pan, L., & Liu, X. (2025). Study of a Visual Measurement System for Woven Grids. *Smart Wearable Technology*. https://doi.org/10.47852/bonviewSWT52025433